nature neuroscience

The calcium-activated chloride channel anoctamin 1 acts as a heat sensor in nociceptive neurons

Hawon Cho[1,8], Young Duk Yang[2,8], Jesun Lee[1], Byeongjoon Lee[1], Tahnbee Kim[1], Yongwoo Jang[1], Seung Keun Back[3], Heung Sik Na[3], Brian D Harfe[4], Fan Wang[5], Ramin Raouf[6], John N Wood[6] & Uhtaek Oh[1,7]

Nociceptors are a subset of small primary afferent neurons that respond to noxious chemical, thermal and mechanical stimuli. Ion channels in nociceptors respond differently to noxious stimuli and generate electrical signals in different ways. Anoctamin 1 (ANO1 also known as TMEM16A) is a Ca^{2+}-activated chloride channel that is essential for numerous physiological functions. We found that ANO1 was activated by temperatures over 44 °C with steep heat sensitivity. ANO1 was expressed in small sensory neurons and was highly colocalized with nociceptor markers, which suggests that it may be involved in nociception. Application of heat ramps to dorsal root ganglion (DRG) neurons elicited robust ANO1-dependent depolarization. Furthermore, knockdown or deletion of ANO1 in DRG neurons substantially reduced nociceptive behavior in thermal pain models. These results indicate that ANO1 is a heat sensor that detects nociceptive thermal stimuli in sensory neurons and possibly mediates nociception.

Nociceptive neural impulses originate in primary afferent neurons in dorsal root or trigeminal ganglia, which then activate neurons in the spinal cord and in specific nuclei in the brain to induce the perception of pain. Sensory transduction in DRG neurons is achieved through the activation of specific classes of ion channels[1]. These channels are molecular sensors that may detect innocuous and noxious stimuli and transduce them into electrical impulses. DRG neurons are heterogeneous in terms of size and response to various stimuli[2]. Small neurons respond specifically to noxious heat, chemical and mechanical stimuli, and are therefore considered to be polymodal nociceptors. Numerous TRP channels are found in nociceptors[3–5] and many are thermal sensors that detect a wide range of thermal stimuli from cold to noxious heat. Perhaps the best example of a heat sensor is TRPV1, which is activated by heat, acid and capsaicin, the pungent ingredient of hot peppers[6,7]. In fact, *Trpv1*$^{-/-}$ mice show reduced thermal hyperalgesia and inflammatory pain[8,9]. On the other hand, TRPV2 is activated by noxious heat over 53 °C and by 2-aminoethoxydiphenyl borate[10,11]. TRPA1 is expressed in nociceptors and responds to environmental irritants, the pungent ingredients of wasabi, mustard oil and garlic[12,13]. TRPA1 is also known to respond to noxious cold[12,14,15]. Other thermoTRPs detect changes in temperature that are outside of the noxious range. Although there is no doubt that TRPV1 is a heat sensor, the presence of additional heat sensors is likely, mainly because avoidance behaviors to heat remain in mice lacking TRPV1 and TRPV1-negative neurons respond to heat[1,9,16].

Ca^{2+}-activated chloride channels (CaCCs) are activated by intracellular Ca^{2+} and mediate numerous physiological functions, such as the epithelial movement of fluid[17]. In addition, endogenous CaCCs are known to regulate sensory transduction for vision, taste, smell and somatic sensations[18]. In terms of visual sensory transduction, CaCCs control Ca^{2+} currents and thereby modulate lateral inhibition in the retina[19,20] or amplify odorant-evoked signals in olfactory sensory neurons[21,22]. ANO1 was recently identified and found to possess eight transmembrane domains and to conduct chloride currents activated by intracellular Ca^{2+} (refs. 23–25). Furthermore, ANO1 has biophysical properties and a pharmacological profile similar to those of endogenous CaCCs[25]. Because ANO1 is expressed in DRG neurons[25], it might reasonably be expected to participate in somatosensory transduction, but its role in somatosensation has not been addressed. Thus, we sought to determine ANO1's role in somatosensation and found that ANO1 was activated by heat. In conjunction with its expression in sensory neurons, ANO1 appears to function as a sensor that mediates or amplifies thermal nociception.

RESULTS

Activation of ANO1 by noxious heat

To determine whether changes in temperature activate ANO1, we recorded whole-cell currents in HEK 293T cells transfected with mouse ANO1 (ANO1-HEK cells) after applying heat ramps to bath solutions. Bath and pipette solutions contained 140 mM NMDG-Cl, which was introduced to ensure that Cl^- was the sole charge carrier. Notably, raising the temperature above 44 °C resulted in robust inward Cl^- currents at a holding potential of −60 mV in ANO1-HEK cells (**Fig. 1a**), whereas heat ramp failed to activate currents in

[1]Sensory Research Center, Creative Research Initiatives, College of Pharmacy, Seoul National University, Seoul, Republic of Korea. [2]Department of Pharmacy, College of Pharmacy, CHA University, Gyeonggi-do, Republic of Korea. [3]Department of Physiology, College of Medicine, Korea University, Seoul, Republic of Korea. [4]Department of Molecular Genetics and Microbiology and the Genetics Institute, University of Florida, College of Medicine, Gainesville, Florida, USA. [5]Department of Cell Biology, Duke University Medical Center, Durham, North Carolina, USA. [6]Molecular Nociception Group, Wolfson Institute for Biomedical Research, University College London, London, UK. [7]Department of Molecular Medicine and Biopharmaceutical Sciences, Graduate School of Convergence Science and Technology, Seoul National University, Seoul, Republic of Korea. [8]These authors contributed equally to this work. Correspondence should be addressed to U.O. (utoh@snu.ac.kr).

Received 3 January; accepted 19 April; published online 27 May 2012; doi:10.1038/nn.3111

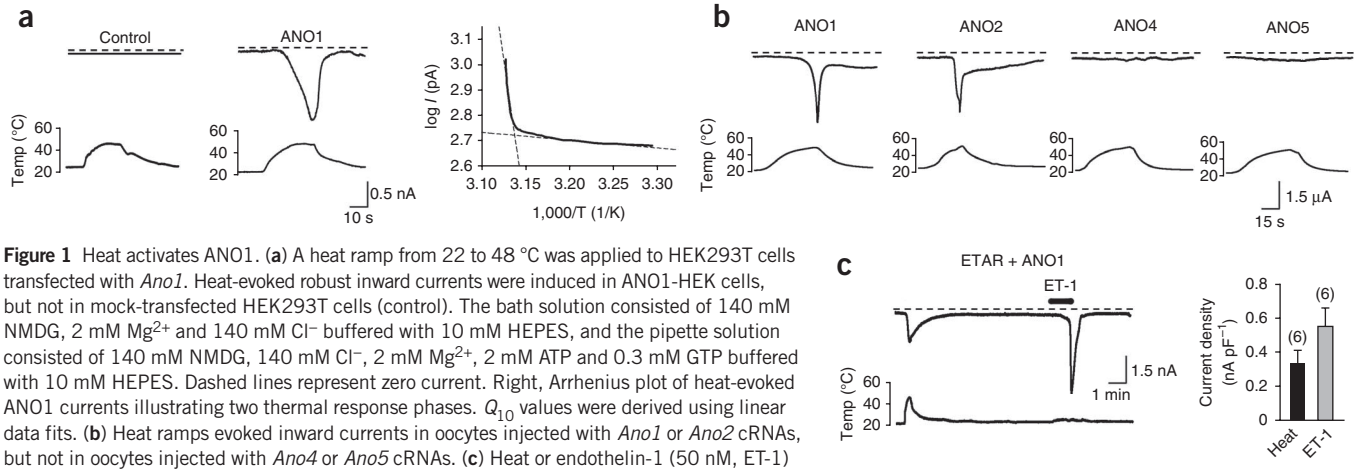

Figure 1 Heat activates ANO1. (**a**) A heat ramp from 22 to 48 °C was applied to HEK293T cells transfected with *Ano1*. Heat-evoked robust inward currents were induced in ANO1-HEK cells, but not in mock-transfected HEK293T cells (control). The bath solution consisted of 140 mM NMDG, 2 mM Mg^{2+} and 140 mM Cl^- buffered with 10 mM HEPES, and the pipette solution consisted of 140 mM NMDG, 140 mM Cl^-, 2 mM Mg^{2+}, 2 mM ATP and 0.3 mM GTP buffered with 10 mM HEPES. Dashed lines represent zero current. Right, Arrhenius plot of heat-evoked ANO1 currents illustrating two thermal response phases. Q_{10} values were derived using linear data fits. (**b**) Heat ramps evoked inward currents in oocytes injected with *Ano1* or *Ano2* cRNAs, but not in oocytes injected with *Ano4* or *Ano5* cRNAs. (**c**) Heat or endothelin-1 (50 nM, ET-1) evoked inward currents in HEK cells transfected with *Ano1* and endothelin receptor subtype A (ETAR, E_{hold} = – 60 mV). Right, summary of heat-induced and receptor-stimulated currents. Error bars represent s.e.m. The numbers of experiments are given in parentheses.

empty vector–transfected (**Fig. 1a**) and non-transfected cells (data not shown). However, temperature increases in the low-to-moderate range (23–42 °C) did not produce current responses in ANO1-HEK cells. Furthermore, the chelation of intracellular Ca^{2+} with 10 mM 1,2-bis(2-amiphenoxy)ethane-*N*,*N*,*N*′,*N*′-tetraacetate (BAPTA) failed to block heat-induced ANO1 currents, ruling out the possibility that heat activates ANO1 indirectly via the release of intracellular Ca^{2+} (**Supplementary Fig. 1a**).

We estimated the 10° temperature coefficient (Q_{10}) of ANO1, which was used to assess its temperature sensitivity, from the linear fit of the log(I) versus 1/T plot[26,27]. When exposed to heat, ANO1 exhibited a steep activation phase (Q_{10} = 19.4 ± 5.9, n = 9) and a shallower phase (Q_{10} = 1.19 ± 0.04, n = 9) (**Fig. 1a**). The thermal threshold (T_h) estimated from the inflection point of these two phases was 44 °C (ref. 27).

The anoctamin family contains ten homologs, but only ANO1 and ANO2 were found to respond to heat (n = 9; **Fig. 1b**). Other ANO channels (ANO4 to ANO7 and ANO10) failed to respond to heat ramps (22–52 °C, n = 5–10; **Fig. 1b**). In addition, ANO1-expressing cells were also found to respond to endothelin-1, a physiological ligand that activates endogenous CaCCs via the phospholipase C/inositol 1,4,5-triphosphate pathway (**Fig. 1c**).

Heat-evoked ANO1 currents in ANO1-HEK cells were outwardly rectifying and reversed at near zero mV (–5.0 mV, n = 5) under symmetric 140 mM NMDG-Cl solution conditions (**Supplementary Fig. 1b**).

To determine the relative permeabilities of heat-induced currents to monovalent anions, we used a pipette solution containing 140 mM NMDG-Cl (0 mM Ca^{2+} with no added EGTA) and a bath solution containing 140 mM NaCl. When NaCl in the bath was substituted with equimolar NaF, NaBr, NaI or $NaNO_3$, the reversal potentials of heat-evoked currents in ANO1-HEK cells shifted from –9.85 ± 2.5 mV (n = 6) to +11.9 ± 4.0 (n = 6), –20.1 ± 1.1 (n = 5), –22.5 ± 1.5 (n = 6) or –27.0 ± 1.9 mV (n = 8), respectively (**Supplementary Fig. 1c**). Thus, the relative permeabilities of these monovalent anions in heat-induced currents of ANO1 followed the order NO_3^- (1.97) > I^- (1.65) > Br^- (1.48) > Cl^- (1.0) > F^- (0.42), which is consistent with the permeabilities of endogenous Ca^{2+}-activated currents[18,28]. Furthermore, heat-evoked ANO1 currents were inhibited by the Cl^- channel blocker mefloquine (5 µM, 90.5 ± 4.4% reduction, n = 5, Student's unpaired two-tailed t test, P < 0.001; **Supplementary Fig. 1d**,**e**). A second application of heat with the control bath solution resulted in weak tachyphylaxis, which elicited a moderate reduction in heat-evoked currents (38.8 ± 6.5% reduction, n = 12). ANO1 was activated by heat in isolated membrane patches. Heat-evoked currents were observed in inside-out patches excised from ANO1-transected HEK293 cells, but not from control HEK cells (**Supplementary Fig. 2**).

Heat has a synergistic effect on the Ca^{2+} response of ANO1

As with many other thermoTRPs whose activation is affected by temperature or voltage changes and by their ligands, ANO1 activation was affected by heat, voltage and its endogenous ligand, Ca^{2+}. When the pipette

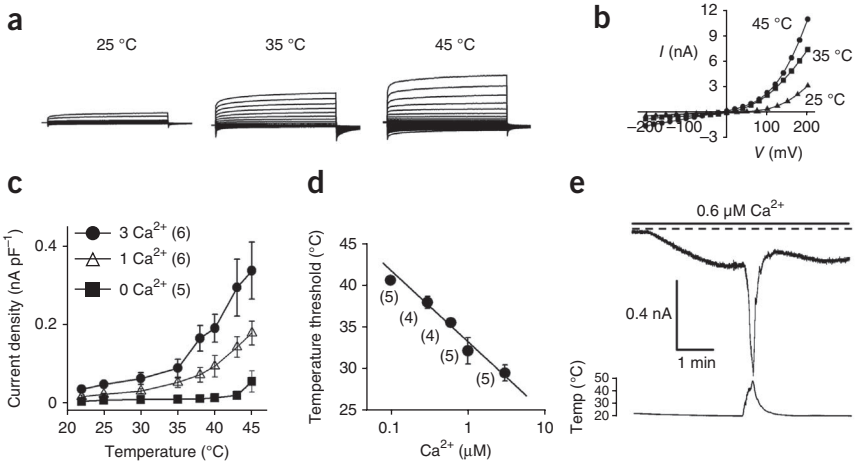

Figure 2 Synergistic effects of heat and Ca^{2+} on ANO1 activation. (**a**) Whole-cell currents of ANO1-HEK cells in response to various bath solution temperatures. Voltage pulses from –200 mV to +200 mV in 25-mV increments were used. The pipette solution contained 140 mM NMDG-Cl without Ca^{2+}. (**b**) I-V curves of ANO1 currents at bath solution temperatures of 25, 35 and 45 °C. (**c**) Ca^{2+} lowered the temperature threshold of heat-induced currents and increased the magnitude of currents in ANO1-HEK cells. (**d**) Temperature thresholds of ANO1 currents applied at different Ca^{2+} concentrations (n = 4–5). (**e**) ANO1 currents activated by 0.6 µM Ca^{2+} were increased by heat.

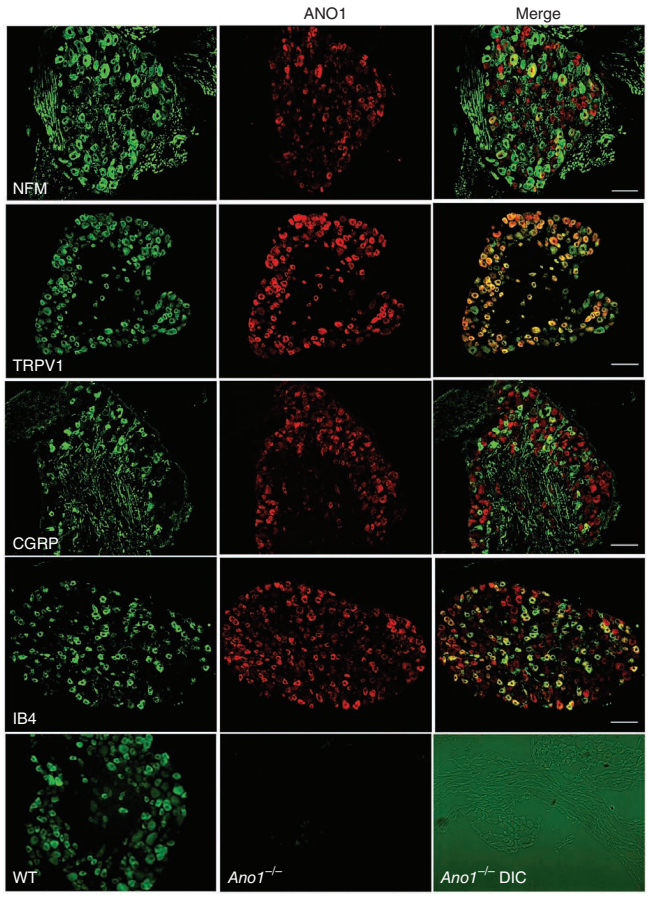

Figure 3 ANO1 is expressed mainly in nociceptors of DRG neurons. Immunofluorescent images of mouse DRG neurons. Thin sections (10 μm) of mouse DRGs were double-stained with antibodies to mouse ANO1 (red), neurofilament M (NFM), TRPV1 (green), CGRP (green) and isolectin B4 (IB4, green). Images are shown at 200× magnification. Scale bars represent 100 μm. WT, wild type. DIC, differential interference contrast.

solution contained 0 mM of Ca^{2+}, ANO1 currents induced by voltage pulses (–200 to +200 mV) increased with bath temperature with a prominent outwardly rectifying current-voltage relationship (**Fig. 2a**,**b**). Increases in intracellular Ca^{2+} concentration ($[Ca^{2+}]_i$) markedly increased heat-induced current densities (**Fig. 2c**). Furthermore, increases in $[Ca^{2+}]_i$ decreased the temperature thresholds required for activating ANO1, such that ANO1 was activated at near body temperature when $[Ca^{2+}]_i$ was increased above 0.1 μM, the $[Ca^{2+}]_i$ present in the resting state (**Fig. 2d**). We also observed synergistic effects between heat and Ca^{2+}, as we found much greater currents when heat and Ca^{2+} (0.6 μM) were applied than when Ca^{2+} was applied alone (0.28 ± 0.05 versus 0.09 ± 0.02 nA pF^{-1}, $n = 8$, Student's unpaired two-tailed t test, $P < 0.01$; **Fig. 2e**). Moreover, the ANO1 response activated by saturating Ca^{2+} (10 μM) was also potentiated by heat (**Supplementary Fig. 3**). Thus, these results suggest that heat, voltage and Ca^{2+} synergistically sensitize each other's effects on ANO1 and that temperatures lower than 44 °C can activate ANO1 at physiological membrane potentials because $[Ca^{2+}]_i$ increases under pathological conditions such as inflammation.

Activation of ANO1 by heat depolarizes DRG neurons

ANO1 was found to be primarily expressed in small-diameter nociceptive neurons. About 78% of ANO1-immunoreactive DRG neurons (399 of 511 neurons) were also immunoreactive for TRPV1, a marker of nociceptors (**Fig. 3**). Moreover, 58.4% of ANO1-positive neurons also expressed isolectin B4, a marker of nonpeptidergic small sensory neurons. In addition, 31.6% of ANO1-expressing neurons were colocalized with calcitonin gene-related peptide (CGRP), a marker of peptidergic small sensory neurons. We also found ANO1 immunoreactivity in larger myelinated neurons, as 25% of ANO1-positive neurons (77 of 311 neurons) also expressed neurofilament M, a marker of myelinated DRG neurons (**Fig. 3**).

We examined whether heat ramps could activate Cl^- conductances in cultured DRG neurons. To measure just Cl^- current, we used 140 mM NMDG-Cl in the pipette and bath solutions. In DRG neurons isolated

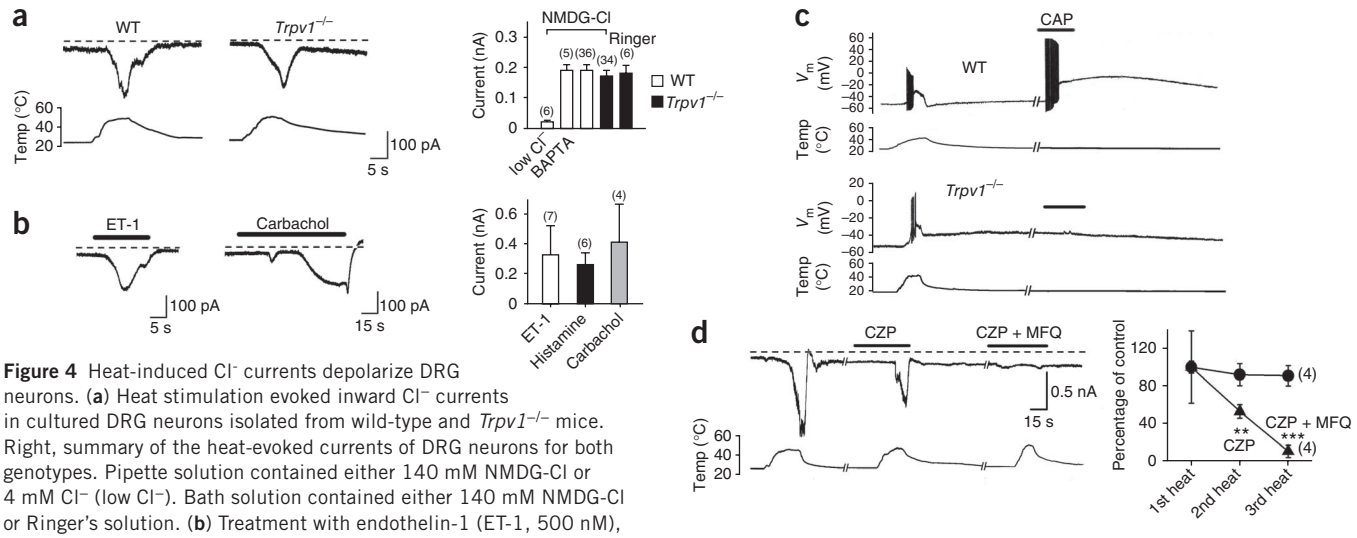

Figure 4 Heat-induced Cl^- currents depolarize DRG neurons. (**a**) Heat stimulation evoked inward Cl^- currents in cultured DRG neurons isolated from wild-type and *Trpv1*$^{-/-}$ mice. Right, summary of the heat-evoked currents of DRG neurons for both genotypes. Pipette solution contained either 140 mM NMDG-Cl or 4 mM Cl^- (low Cl^-). Bath solution contained either 140 mM NMDG-Cl or Ringer's solution. (**b**) Treatment with endothelin-1 (ET-1, 500 nM), carbachol (2 mM) or histamine (1 mM) evoked inward Cl^- currents in DRG neurons isolated from mice. Right, summary of ligand-evoked currents. (**c**) Heat markedly depolarized DRG neurons from wild-type and *Trpv1*$^{-/-}$ mice. The TRPV1 agonist capsaicin (CAP) strongly depolarized DRG neurons from wild-type mice, but not those from *Trpv1*$^{-/-}$ mice. (**d**) Inhibition of heat-induced inward currents by a TRPV1 antagonist (10 μM capsazepine, CZP) and a CaCC blocker (100 μM mefloquine, MFQ) in the DRG neurons of wild-type mice. Right, summary of the inhibition of heat-induced inward currents by CZP or MFQ. $^{**}P < 0.01$, $^{***}P < 0.001$ (one-way ANOVA followed by Tukey's *post hoc* tests). Error bars represent ± s.e.m.

from wild-type and *Trpv1*$^{-/-}$ mice, a heat ramp from 23 to 48 °C evoked inward Cl^- currents (**Fig. 4a**). In addition, heat-induced inward currents were still observed after chelating intracellular Ca^{2+} with 10 mM BAPTA in the pipette solution (**Fig. 4a**). However, lowering intracellular chloride concentration (4 mM) with 140 mM of potassium aspartate pipette solution almost completely reduced the heat-induced inward currents (**Fig. 4a**). These heat-induced currents in DRG neurons from *Trpv1*$^{-/-}$ mice were also observed in physiologically relevant Ringer's solution (**Fig. 4a**). Furthermore, heat-induced currents in DRG neurons isolated from *Trpv1*$^{-/-}$ mice had a temperature sensitivity and threshold similar to those of heterologously expressed ANO1 (steep phase $Q_{10} = 24.4 \pm 13.8$, shallow phase $Q_{10} = 1.3 \pm 0.2$; $n = 6$). The temperature threshold obtained from the intersection of the two phases was 44.1 °C.

These inward Cl^- currents in DRG neurons were activated by inflammatory mediators, such as endothelin-1, carbachol or histamine, which are known to excite DRG neurons and thereby evoke pain or itch[29,30] (**Fig. 4b**). Furthermore, these ligands are also known to stimulate endogenous CaCCs via the phospholipase C/inositol 1,4,5-triphosphate pathway[28,31]. Thus, these results suggest that heat and endogenous mediators can evoke Cl^- currents in DRG neurons.

Because ANO1 is a Cl^- channel, it is questionable whether its activation excites sensory neurons. An increase in Cl^- conductance can lead to the depolarization or hyperpolarization of cells depending on the intracellular Cl^- concentration. Direct measurements of Cl^- concentration in DRG neurons indicate that its concentration is ≥~30 mM (refs. 32,33). Thus, the pipette solution was set at 30 mM Cl^- and the bath solution at 140 mM NaCl. In these salt conditions, current-clamp recordings of DRG neurons of wild-type mice exhibited robust depolarization (33.7 ± 3.2 mV, $n = 5$) by the heat ramp from the resting membrane potential (-53.6 ± 1.1 mV, $n = 5$) (**Fig. 4c**). Capsaicin, a TRPV1 agonist, also evoked depolarizations in the DRG neurons of wild-type mice. However, although the heat ramp produced comparable depolarization in the DRG neurons of mice lacking TRPV1 (27.24 ± 3.11 mV, $n = 5$), capsaicin had no effect (wild type, 38.1 ± 2.2 mV; *Trpv1*$^{-/-}$, 5.0 ± 0.6 mV; $n = 5$, Student's unpaired two-tailed *t* test, $P < 0.001$; **Fig. 4c**). These results indicate that the opening of Cl^- channels via heat ramps can depolarize DRG neurons. However, there was no difference in the membrane potential (V_m) change evoked by heat between the two genotypes. There was a clear difference in the spiking frequency evoked by the heat ramp, such that the frequency of action potential spikes of DRG neurons from wild-type mice was significantly greater than those of DRG neurons from *Trpv1*$^{-/-}$ mice (wild type, 28.4 ± 3.2 spikes per s; *Trpv1*$^{-/-}$, 12 ± 2.5 spikes per s; $n = 7$–10, Student's unpaired two-tailed *t* test, $P < 0.01$; **Fig. 4c**), which suggests that TRPV1 contributes to action potential generation. The relative contributions of TRPV1 and ANO1 were also examined by treating DRG neurons with inhibitors specific for TRPV1 and ANO1 under physiological solution conditions. A competitive TRPV1 antagonist, capsazepine (10 μM), substantially blocked heat-induced currents (**Fig. 4d**). Co-treatment with capsazepine and 100 μM mefloquine, an antagonist of endogenous CaCCs, almost completely inhibited heat-induced currents. Consistent with this, heat-evoked currents in DRG cells from *Trpv1*$^{-/-}$ mice were blocked by mefloquine (**Supplementary Fig. 4a**). In contrast, mefloquine treatment alone failed to block heat-evoked currents in HEK cells transfected with TRPV1 (**Supplementary Fig. 4b**).

We found that ANO2 was also activated by heat (**Fig. 1b**). Thus, ANO2 could also contribute to the Cl^- currents induced by heat in DRG neurons. However, ANO1 is largely responsible for the heat-induced Cl^- currents in DRG neurons, as the transcript level of *Ano2* in DRG cells was about tenfold lower than that of ANO1 (**Supplementary Fig. 5**).

Thermal nociception of ANO1 siRNA-treated mice

The activation of ANO1 in the noxious temperature range and its expression in small DRG neurons suggest its involvement in nociception. We therefore used behavioral assays to investigate whether ANO1 mediates heat-induced nociception. First, we examined whether the pharmacological inhibition of ANO1 has an anti-nocifensive effect on noxious thermal stimuli. The administration of mefloquine (40 mg per kg of body weight) significantly increased tail-withdrawal latency from radiant heat as compared with saline-treated control rats (saline, 4.2 ± 0.5 s; mefloquine, 9.5 ± 2.1 s; $n = 6$–7, $P < 0.05$, Student's unpaired two-tailed *t* test). When hindpaw inflammation was induced by intraplantar injections of carrageenan, the hindpaw withdrawal latency from radiant heat was significantly decreased (**Fig. 5a**). However, animals pretreated with mefloquine failed to

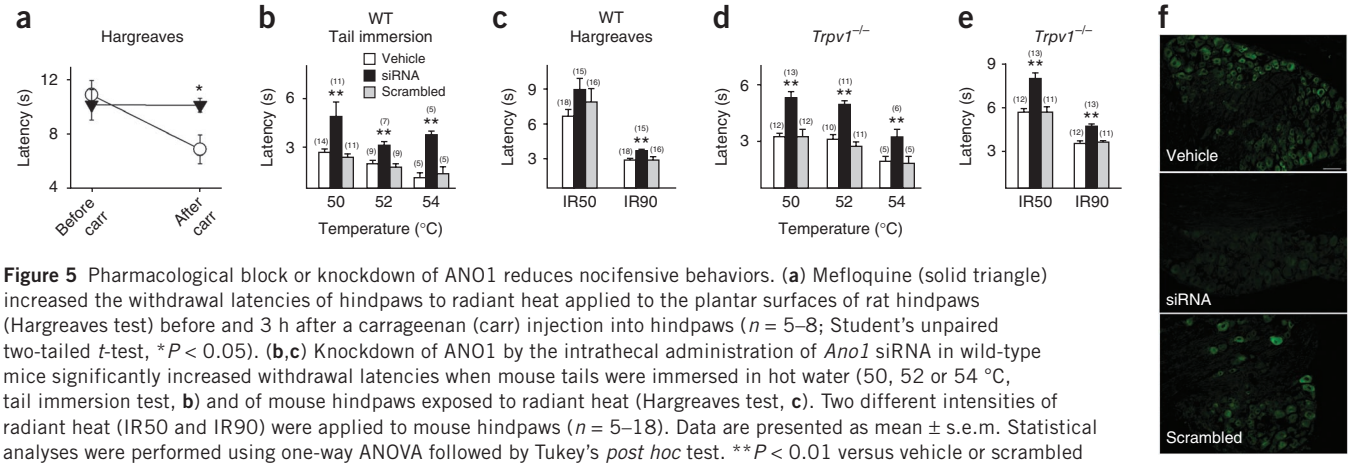

Figure 5 Pharmacological block or knockdown of ANO1 reduces nocifensive behaviors. (**a**) Mefloquine (solid triangle) increased the withdrawal latencies of hindpaws to radiant heat applied to the plantar surfaces of rat hindpaws (Hargreaves test) before and 3 h after a carrageenan (carr) injection into hindpaws ($n = 5$–8; Student's unpaired two-tailed *t*-test, $^*P < 0.05$). (**b**,**c**) Knockdown of ANO1 by the intrathecal administration of *Ano1* siRNA in wild-type mice significantly increased withdrawal latencies when mouse tails were immersed in hot water (50, 52 or 54 °C, tail immersion test, **b**) and of mouse hindpaws exposed to radiant heat (Hargreaves test, **c**). Two different intensities of radiant heat (IR50 and IR90) were applied to mouse hindpaws ($n = 5$–18). Data are presented as mean ± s.e.m. Statistical analyses were performed using one-way ANOVA followed by Tukey's *post hoc* test. $^{**}P < 0.01$ versus vehicle or scrambled siRNA–treated controls. (**d**,**e**) The intrathecal administration of *Ano1* siRNA in *Trpv1*$^{-/-}$ mice significantly increased tail immersion withdrawal latencies (at 50, 52 or 54 °C, **d**) and Hargreaves test latencies ($n = 5$–13, **e**). All data represent mean ± s.e.m. Statistical analyses were performed using one-way ANOVA followed by Tukey's *post hoc* test. $^{**}P < 0.01$ versus vehicle or scrambled siRNA–treated controls. (**f**) The number of ANO1-expressing neurons and their immunofluorescent intensity were markedly reduced in DRG neurons isolated from *Ano1* siRNA–treated mice. DRG neurons from vehicle, siRNA-treated and scrambled siRNA–treated mice were stained with antibodies to mouse ANO1 (green). Images are shown at 200× magnification. Scale bar represents 50 μm.

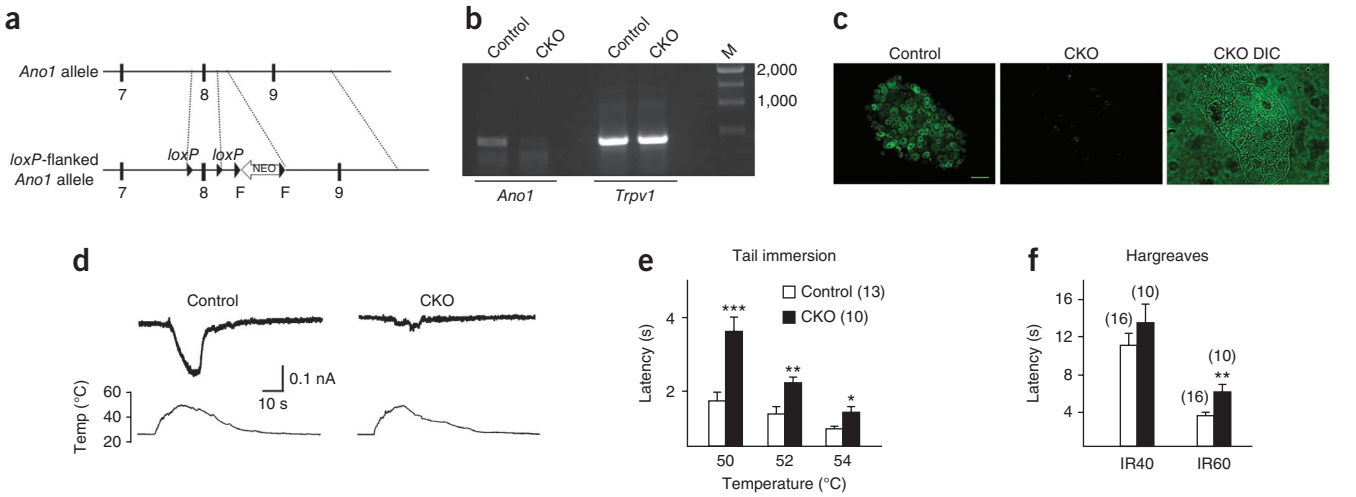

Figure 6 Conditional knockout of ANO1 in DRGs reduces thermal hyperalgesia. (**a**) Gene targeting strategy. Exon 8 in the *Ano1* locus is flanked with two *loxP* sites (arrowheads) followed by a FRT-flanked neo cassette (neo and F). To ablate *Ano1* in DRG neurons, we crossed $Ano1^{loxP/+}$ mice with $Avil^{cre}$ mice to eventually obtain $Avil^{cre}$-$Ano1^{loxP/loxP}$ (ANO1 CKO) mice and littermate controls ($Avil^{cre}$-$Ano1^{+/+}$) (see Online Methods). (**b**) Reverse-transcription PCR analysis of *Ano1* and *Trpv1* expression in control and conditional knockout mice (CKO). (**c**) Immunofluorescent images of sections of DRG neurons isolated from control and CKO mice stained with antibody to ANO1. Images are shown at 200× magnification. Scale bar represents 50 μm. (**d**) Whole-cell currents were recorded in primary cultured DRG neurons isolated from control and CKO mice. Although control mice showed Cl^- currents induced by heat (left), heat-evoked response was significantly reduced in CKO mice ($n = 7$). (**e**,**f**) Ablation of ANO1 from DRG neurons from CKO mice significantly increased withdrawal latencies when mouse tails were immersed in hot water (50, 52 or 54 °C, **e**) and of mouse hindpaws exposed to radiant heat (**f**). Two different intensities of radiant heat (IR40 and IR60) were applied to mouse hindpaws ($n = 10$–16). All data represent mean ± s.e.m. Statistical analyses were performed using Student's unpaired two-tailed *t*-test. $^*P < 0.05$, $^{**}P < 0.01$ and $^{***}P < 0.001$ versus control mice.

demonstrate the heat-induced hyperalgesia. On the other hand, the analgesic effect of mefloquine was not observed in mechanical pain tests. In particular, mefloquine failed to block inflammation-induced mechanical allodynia or hyperalgesia in the Von Frey hair or Randal Selitto test (**Supplementary Fig. 6**).

We used small interfering RNA (siRNA) specific for *Ano1* to investigate whether ANO1 knockdown has an anti-nociceptive effect. Significant increases in tail-withdrawal latency from 50–54 °C water were observed in mice treated intrathecally with ANO1 siRNA (**Fig. 5b**), whereas intrathecal scrambled siRNA did not alter tail-withdrawal latency. Similarly, in the Hargreaves test, intrathecal ANO1 siRNA–treated in mice also elicited a significant increase in withdrawal latency from radiant heat with the higher of the two intensities tested (IR90; **Fig. 5c**). We examined ANO1 activity in dissociated sensory neurons from siRNA-treated mice. Heat ramps evoked significantly smaller currents in DRG neurons isolated from mice treated with ANO1 siRNA than those treated with scrambled siRNA (**Supplementary Fig. 7**; $P < 0.01$). To exclude the thermal response mediated by TRPV1, we performed identical behavioral assays using $Trpv1^{-/-}$ mice. ANO1 siRNA treatment in $Trpv1^{-/-}$ mice induced a significant increase in tail-withdrawal latency from hot water (50–54 °C; **Fig. 5d**). In the Hargreaves test, intrathecal ANO1 siRNA in $Trpv1^{-/-}$ mice also induced significant increases in withdrawal latency from radiant heat at both intensities (**Fig. 5e**). Immunofluorescence staining revealed that ANO1 expression was markedly reduced in DRG neurons of mice treated with ANO1 siRNA (**Fig. 5f**). Taken together, these results suggest that ANO1 contributes to heat-evoked nociception and inflammation-induced thermal hyperalgesia.

Thermal nociception in ANO1 conditional knockout mice

Complete deletion of ANO1 causes severe respiratory problems and poor growth, resulting in death in early neonatal period[34]. Thus, tissue-specific ANO1 disruption is needed to study the functional role of ANO1 in thermal pain sensation. For this, we generated *Ano1* conditional knockout mice using mice that express Cre recombinase under the control of the *Avil* (advillin) promoter ($Avil^{cre}$). Advillin is a member of the gelsolin superfamily of actin-binding proteins and is expressed exclusively in trigeminal and DRG neurons[35,36]. Thus, $Avil^{cre}$ is a suitable tool for examining ANO1 function in all primary afferent neurons. To make an ANO1 conditional knockout (CKO) in DRG neurons, we generated $Ano1^{loxP/+}$ mice by flanking exon 8 of *Ano1* with *loxP* sites using homologous recombination in embryonic stem cells (Online Methods and **Fig. 6a**). To ablate ANO1 specifically in DRG neurons, we crossed $Ano1^{loxP/+}$ mice with $Avil^{cre}$ and obtained ANO1 CKO ($Avil^{cre}$; $Ano1^{loxP/loxP}$) mice and littermate controls ($Avil^{cre}$; $Ano1^{+/+}$). *Ano1* transcript levels in DRGs isolated from ANO1 CKO mice were markedly reduced compared with those of control mice. However, there was no difference in *Trpv1* transcript levels between control mice and ANO1 CKO mice (**Fig. 6b**). Furthermore, ANO1-containing neurons were visible in DRGs isolated from control mice, whereas very few cells to none were visible in DRG isolated from ANO1 CKO mice (**Fig. 6c**). We found no differences in balance, motor coordination and locomotion between control and ANO1 CKO mice (**Supplementary Fig. 8**).

If ANO1 is a functional heat sensor, its removal from DRG neurons should lead to a reduction in heat-sensitive Cl^- currents. Indeed, a heat ramp from 23 to 48 °C evoked an inward Cl^- current in DRG neurons isolated from control mice. However, the heat-evoked inward Cl^- current was markedly decreased in ANO1 CKO mice (control, 0.21 ± 0.02 nA; ANO1 CKO, 0.04 ± 0.01 nA; $n = 6$–7, $P < 0.01$, Student's unpaired two-tailed *t* test; **Fig. 6d**). Furthermore, as observed in *Ano1* siRNA treatments, ANO1 CKO mice exhibited a pronounced analgesic effect in response to heat, but not mechanical, stimuli. Ablation of ANO1 in DRG neurons resulted in a marked increase in tail-withdrawal latency compared with control mice when tails were submerged in 50–54 °C water (**Fig. 6e**). In the Hargreaves

test, ANO1 CKO mice also elicited a significant increase in withdrawal latency from radiant heat with the higher of the two intensities tested (IR60; **Fig. 6f**). In contrast, when tested by Von Frey hairs, mechanical sensitivities were not different between the two genotypes (0.36 ± 0.1 g control versus 0.39 ± 0.15 g CKO, $n = 7–13$, $P < 0.839$, Student's unpaired two-tailed t test).

DISCUSSION

Nociceptors express many different channels that confer sensitivity to mechanical stimuli, heat, cold and chemicals[1,3,4]. Because they express channels of multiple modes, nociceptors are often referred to as being polymodal. The differential expression of these channels in primary afferent neurons results in a rich repertoire of pain sensations. Since the discovery of the TRP channel family, great progress has been made in the understanding of some of the molecular mechanisms of thermosensation[3–5]. Many thermoTRPs respond to diverse thermal stimuli and are probably the molecular sensors responsible for the detection of different temperatures. Of these, TRPV1 is the best known for detecting noxious heat[6,8], although the presence of additional heat sensors has been suggested[1,16]. We found that ANO1 becomes activated at temperatures exceeding 44 °C. ANO1 was largely expressed in nociceptors, and pharmacological block or deletion of *Ano1* markedly attenuated nocifensive behaviors in response to heat. Thus, ANO1 appears to be a candidate heat sensor in nociceptors.

Because ANO1 is a Cl^- channel, the opening of ANO1 can lead to the hyperpolarization or depolarization of neurons in an intracellular chloride concentration ($[Cl^-]_i$)-dependent manner. $[Cl^-]_i$ in DRG neurons is regulated primarily by the sodium-potassium-chloride co-transporter 1 (NKCC1), which accumulates Cl^- in cells[37]. Thus, unlike neurons in the CNS, DRG neurons maintain higher $[Cl^-]_i$ levels than are present during electrochemical equilibrium because of elevated NKCC1 expression and activity[38]. The equilibrium potential of Cl^- is far more positive (–27 mV) than the resting membrane potential (–60 to –55 mV) in DRG neurons[32,33,38]; thus, the activation of Cl^- channels in DRG neurons leads to depolarization. The most well-known example of this phenomenon is the depolarization of the central terminals of DRG neurons by $GABA_A$ receptor activation, which causes primary afferent depolarization of nociceptive afferent fibers, a classical type of presynaptic inhibition of dorsal horn neurons in the spinal cord by large primary afferent fibers[38,39]. Depolarization by GABA is not confined to the central terminals of DRG neurons, but is also found in cell bodies and in peripheral terminals[40]. Notably, the activation of endogenous CaCCs by an increase in $[Cl^-]_i$ is known to depolarize sensory neurons[17,18,41]. We found that pain- or itch-causing substances, such as carbachol, endothelin 1 and histamine, which are known to increase intracellular Ca^{2+}, evoked Cl^--based inward currents. Furthermore, NKCC1 blockers have been reported to reduce histamine-induced itch and flare in humans[42]. These findings suggest that ANO1 is an important element that generates or controls nociceptive signal transduction in sensory neurons.

Recently, two other heat-sensitive molecules have been described as additional noxious heat sensors[43,44]. One is the TRPM3 channel, a member of the melastatin subfamily of TRP channels. TRPM3 is widely expressed in neuronal and non-neuronal tissues, and is potentially activated by pregnenolone sulfate. It was recently reported that TRPM3 responds to thermal stimuli (>40 °C). In addition, TRPM3-deficient mice exhibit impaired responses to noxious heat[43]. STIM1 is an endoplasmic reticulum Ca^{2+} sensor that rapidly translocates to couple with Ca^{2+}-permeable Orai1 channels following Ca^{2+} store depletion[45]. A recent study found that STIM1 is also activated by changes in temperature without store depletion, leading to Orai1-mediated Ca^{2+} influx[44]. Heat causes clustering of STIM1 and leads to Orai1-mediated influx as a heat-off response (cooling after heat). Although these two proteins are heat sensitive, it is less likely that the ANO1 activation by heat is mediated by STIM1 or TRPM3, as the level of *Trpm3* transcripts was undetectable in GFP- and ANO1-transfected HEK cells and the level of *Stim1* transcripts was not changed by ANO1 transfection (**Supplementary Fig. 9**). In addition, ANO1 was activated by heat in excised membrane patches where the endoplasmic reticulum was removed (**Supplementary Fig. 2**). Thus, activation of ANO1 by heat cannot be dependent on STIM1. Together, these results suggest that activation of ANO1 by heat is not dependent on activation of TRPM3 or STIM1.

In conclusion, we found ANO1 to be sensitive to noxious heat and to be expressed preferentially in nociceptors. Heat-induced opening of ANO1 depolarized DRG neurons. In addition, pharmacological block or deletion of *Ano1* was found to reduce thermal hyperalgesia. ANO1 agonists are considered to be useful for treating cystic fibrosis. Our results suggest that consideration should be made for the possibility that ANO1 agonists may induce painful side effects when developed for the treatment of cystic fibrosis.

METHODS

Methods and any associated references are available in the online version of the paper.

Note: Supplementary information is available in the online version of the paper.

ACKNOWLEDGMENTS

This work was supported by the World Class University project (R31-2011-00101030), the Creative Research Initiatives Program (20120001246) and a grant (2011K000275) from the Brain Research Center of the 21st Century Frontier Research Program funded by of the Ministry of Education and Science and Technology and the National Research Foundation of the Republic of Korea.

AUTHOR CONTRIBUTIONS

H.C. carried out the patch clamp and behavioral studies and analyzed data. Y.D.Y. and Y.J. performed molecular biological work. J.L. and T.K. performed patch-clamp recordings. B.L., F.W., R.R. and J.N.W. generated CKO mice. S.K.B. and H.S.N. carried out behavioral studies. B.D.H. generated ANO1 systemic knockout mice. U.O. wrote the manuscript and supervised the project.

COMPETING FINANCIAL INTERESTS

The authors declare no competing financial interests.

Published online at http://www.nature.com/doifinder/10.1038/nn.3111.
Reprints and permissions information is available online at http://www.nature.com/reprints/index.html.

1. Basbaum, A.I., Bautista, D.M., Scherrer, G. & Julius, D. Cellular and molecular mechanisms of pain. *Cell* **139**, 267–284 (2009).
2. Perl, E.R. Ideas about pain, a historical view. *Nat. Rev. Neurosci.* **8**, 71–80 (2007).
3. Caterina, M.J. Transient receptor potential ion channels as participants in thermosensation and thermoregulation. *Am. J. Physiol. Regul. Integr. Comp. Physiol.* **292**, R64–R76 (2007).
4. Dhaka, A., Viswanath, V. & Patapoutian, A. Trp ion channels and temperature sensation. *Annu. Rev. Neurosci.* **29**, 135–161 (2006).
5. Talavera, K., Nilius, B. & Voets, T. Neuronal TRP channels: thermometers, pathfinders and life-savers. *Trends Neurosci.* **31**, 287–295 (2008).
6. Caterina, M.J. *et al.* The capsaicin receptor: a heat-activated ion channel in the pain pathway. *Nature* **389**, 816–824 (1997).
7. Tominaga, M. *et al.* The cloned capsaicin receptor integrates multiple pain-producing stimuli. *Neuron* **21**, 531–543 (1998).
8. Caterina, M.J. *et al.* Impaired nociception and pain sensation in mice lacking the capsaicin receptor. *Science* **288**, 306–313 (2000).
9. Davis, J.B. *et al.* Vanilloid receptor-1 is essential for inflammatory thermal hyperalgesia. *Nature* **405**, 183–187 (2000).
10. Caterina, M.J., Rosen, T.A., Tominaga, M., Brake, A.J. & Julius, D. A capsaicin-receptor homologue with a high threshold for noxious heat. *Nature* **398**, 436–441 (1999).

11. Hu, H.Z. *et al.* 2-aminoethoxydiphenyl borate is a common activator of TRPV1, TRPV2 and TRPV3. *J. Biol. Chem.* **279**, 35741–35748 (2004).
12. Jordt, S.E. *et al.* Mustard oils and cannabinoids excite sensory nerve fibres through the TRP channel ANKTM1. *Nature* **427**, 260–265 (2004).
13. Macpherson, L.J. The pungency of garlic: activation of TRPA1 and TRPV1 in response to allicin. *Curr. Biol.* **15**, 929–934 (2005).
14. Karashima, Y. *et al.* TRPA1 acts as a cold sensor *in vitro* and *in vivo*. *Proc. Natl. Acad. Sci. USA* **106**, 1273–1278 (2009).
15. Story, G.M. *et al.* ANKTM1, a TRP-like channel expressed in nociceptive neurons, is activated by cold temperatures. *Cell* **112**, 819–829 (2003).
16. Woodbury, C.J. *et al.* Nociceptors lacking TRPV1 and TRPV2 have normal heat responses. *J. Neurosci.* **24**, 6410–6415 (2004).
17. Hartzell, C., Putzier, I. & Arreola, J. Calcium-activated chloride channels. *Annu. Rev. Physiol.* **67**, 719–758 (2005).
18. Frings, S., Reuter, D. & Kleene, S.J. Neuronal Ca^{2+} -activated Cl^- channels—homing in on an elusive channel species. *Prog. Neurobiol.* **60**, 247–289 (2000).
19. Cia, D. *et al.* Voltage-gated channels and calcium homeostasis in mammalian rod photoreceptors. *J. Neurophysiol.* **93**, 1468–1475 (2005).
20. Lalonde, M.R., Kelly, M.E. & Barnes, S. Calcium-activated chloride channels in the retina. *Channels (Austin)* **2**, 252–260 (2008).
21. Kleene, S.J. High-gain, low-noise amplification in olfactory transduction. *Biophys. J.* **73**, 1110–1117 (1997).
22. Lowe, G. & Gold, G.H. Nonlinear amplification by calcium-dependent chloride channels in olfactory receptor cells. *Nature* **366**, 283–286 (1993).
23. Caputo, A. *et al.* TMEM16A, a membrane protein associated with calcium-dependent chloride channel activity. *Science* **322**, 590–594 (2008).
24. Schroeder, B.C., Cheng, T., Jan, Y.N. & Jan, L.Y. Expression cloning of TMEM16A as a calcium-activated chloride channel subunit. *Cell* **134**, 1019–1029 (2008).
25. Yang, Y.D. *et al.* TMEM16A confers receptor-activated calcium-dependent chloride conductance. *Nature* **455**, 1210–1215 (2008).
26. Voets, T. & Nilius, B. TRPs make sense. *J. Membr. Biol.* **192**, 1–8 (2003).
27. Vyklický, L. *et al.* Temperature coefficient of membrane currents induced by noxious heat in sensory neurones in the rat. *J. Physiol. (Lond.)* **517**, 181–192 (1999).
28. Large, W.A. & Wang, Q. Characteristics and physiological role of the Ca^{2+}-activated Cl^- conductance in smooth muscle. *Am. J. Physiol.* **271**, C435–C454 (1996).
29. Hans, G., Deseure, K. & Adriaensen, H. Endothelin-1-induced pain and hyperalgesia: a review of pathophysiology, clinical manifestations and future therapeutic options. *Neuropeptides* **42**, 119–132 (2008).
30. Lang, P.M. Characterization of neuronal nicotinic acetylcholine receptors in the membrane of unmyelinated human C-fiber axons by *in vitro* studies. *J. Neurophysiol.* **90**, 3295–3303 (2003).
31. Zholos, A. Ca^{2+}- and volume-sensitive chloride currents are differentially regulated by agonists and store-operated Ca^{2+} entry. *J. Gen. Physiol.* **125**, 197–211 (2005).
32. Kaneko, H., Putzier, I., Frings, S. & Gensch, T. Determination of intracellular chloride concentration in dorsal root ganglion neurons by fluorescence lifetime imaging. in *Calcium-Activated Chloride Channels* (ed. Fuller, C.M.) 167–189 (Academic, San Diego, 2002).
33. Rocha-González, H.I., Mao, S. & Alvarez-Leefmans, F.J. Na^+, K^+, $2Cl^-$ cotransport and intracellular chloride regulation in rat primary sensory neurons: thermodynamic and kinetic aspects. *J. Neurophysiol.* **100**, 169–184 (2008).
34. Rock, J.R., Futtner, C.R. & Harfe, B.D. The transmembrane protein TMEM16A is required for normal development of the murine trachea. *Dev. Biol.* **321**, 141–149 (2008).
35. Shibata, M. *et al.* Type F scavenger receptor SREC-I interacts with advillin, a member of the gelsolin/villin family, and induces neurite-like outgrowth. *J. Biol. Chem.* **279**, 40084–40090 (2004).
36. Hasegawa, H., Abbott, S., Han, B.X., Qi, Y. & Wang, F. Analyzing somatosensory axon projections with the sensory neuron–specific *Advillin* gene. *J. Neurosci.* **27**, 14404–14414 (2007).
37. Price, T.J., Cervero, F., Gold, M.S., Hammond, D.L. & Prescott, S.A. Chloride regulation in the pain pathway. *Brain Res. Rev.* **60**, 149–170 (2009).
38. Alvarez-Leefmans, F.J. Chloride transporters in presynaptic inhibition, pain and neurogenic inflammation. in *Physiology and Pathology of Chloride Transporters and Channels in the Nervous System* (eds. Alvarez-Leefmans, F.J. & Delpire, E.) 439–470 (Academic, London, 2009).
39. Willis, W.D. John Eccles' studies of spinal cord presynaptic inhibition. *Prog. Neurobiol.* **78**, 189–214 (2006).
40. Labrakakis, C., Tong, C.K., Weissman, T., Torsney, C. & MacDermott, A.B. Localization and function of ATP and $GABA_A$ receptors expressed by nociceptors and other postnatal sensory neurons in rat. *J. Physiol. (Lond.)* **549**, 131–142 (2003).
41. Scott, R.H., Sutton, K.G., Griffin, A., Stapleton, S.R. & Currie, K.P. Aspects of calcium-activated chloride currents: a neuronal perspective. *Pharmacol. Ther.* **66**, 535–565 (1995).
42. Willis, E.F., Clough, G.F. & Church, M.K. Investigation into the mechanisms by which nedocromil sodium, frusemide and bumetanide inhibit the histamine-induced itch and flare response in human skin *in vivo*. *Clin. Exp. Allergy* **34**, 450–455 (2004).
43. Vriens, J. *et al.* TRPM3 is a nociceptor channel involved in the detection of noxious heat. *Neuron* **70**, 482–494 (2011).
44. Xiao, B., Coste, B., Mathur, J. & Patapoutian, A. Temperature-dependent STIM1 activation induces Ca^{2+} influx and modulates gene expression. *Nat. Chem. Biol.* **7**, 351–358 (2011).
45. Zhang, S.L. *et al.* STIM1 is a Ca^{2+} sensor that activates CRAC channels and migrates from the Ca^{2+} store to the plasma membrane. *Nature* **437**, 902–905 (2005).

ONLINE METHODS

Heterologous expression of ANO1. To induce ANO1 expression in HEK293 cells, we transfected cells with mouse *Ano1* cDNA mixed with FuGene HD (Roche Diagnostics) transfection reagent. Transfected cells were plated onto glass coverslips. Their current responses were recorded 24 to 48 h after transfection.

siRNA. The sets of *Ano1* siRNAs and scrambled siRNA have been previously described[25]. Briefly, to reduce transfection toxicity and efficiently deliver siRNAs to DRGs *in vivo*, we mixed *Ano1* siRNAs with Invivofectamine reagent (Invitrogen) according to the manufacturer's instructions. siRNAs and Invivofectamine (5 μg of the siRNA mixture in 20 μl of 5% (wt/vol) glucose solution) were injected into the L4-L5 lumbar region of 8–10-week-old male C57BL/6J mice under anesthesia. siRNAs were injected with 24-h intervals for 3 consecutive days. We performed behavioral tests 1 d after the last siRNA injection. Gene knockdown in DRGs were confirmed by immunofluorescence of ANO1 staining in DRG neurons.

Reverse-transcription PCR. Total RNAs were isolated by Easy-spin (iNtRON, Biotech) kit from DRGs of ANO1 CKO and wild-type mice. First-strand cDNAs were transcribed by Transcriptor First Strand cDNA Synthesis Kits (Roche Diagnostics) using oligo(dT)18 primer. Reverse-transcription PCR was performed using *Ano1* exon 8–specific amplifying primers (mANO1_CKO_F, TACTCAGCTGCATACCCTCT; mANO1_CKO_R, GGCCATAAACACAGAGAAGA).

Generation of ANO1 CKO mice. The *Ano1* targeting construct was built by conventional cloning. In the construct, exon 8 was flanked by *loxP* sites followed by a FRT-flanked neo cassette. The targeting vector was linearized and inserted into embryonic stem cells (Sv129/R1) with electroporation. Neomycin-resistant cells were selected with geneticin (G418). The positive clones were confirmed by Southern blot analysis using a probe after digestion with *sacI*. Cloned embryonic stem cells were injected to blastocysts of C57BL/6 mice, which produced a large number of chimeric mice. To generate heterozygous mice carrying one *loxP*-flanked allele ($Ano1^{loxP/+}$), we bred these chimeric mice with C57BL/6 mice. The neo cassette was removed by crossing $Ano1^{loxP/+}$ mice with Deleter-FlpE mice (Jackson Laboratory, stock 003800). $Ano1^{loxP/+}$ mice without a neo cassette were then crossed with $Avil^{cre}$ mice to produce $Avil^{cre}$; $Ano1^{loxP/+}$ mice. The $Avil^{cre}$; $Ano1^{loxP/+}$ mice were crossed with $Ano1^{loxP/+}$ mice to generate ANO1-deficient mice ($Avil^{cre}$; $Ano1^{loxP/loxP}$).

Primary DRG neuron cultures. Primary cell cultures of DRG neurons were conducted as previously described[46]. Thoracic and lumbar DRGs were dissected from wild-type, $Trpv1^{-/-}$ and CKO mice, and collected in cold culture medium (4 °C) containing a mixture of DMEM and F-12 solution, 10% (vol/vol) fetal bovine serum (Gibco BRL), 1 mM sodium pyruvate, 50–100 ng ml^{-1} nerve growth factor (Alomon) and 100 units per ml of penicillin/streptomycin. Ganglia were washed with culture medium and incubated for 30 min in a warm (37 °C) DMEM/F-12 mixture containing 1 mg ml^{-1} collagenase (Type II, Worthington Biomedical). DRGs were then washed three times with Mg^{2+}- and Ca^{2+}-free Hank's solution, and incubated with gentle shaking in Hank's solution containing 2.5 mg ml^{-1} of trypsin (Roche Diagnostics) for 30 min at 37 °C. The trypsin-containing solution was then centrifuged at 100 *g* for 10 min. The pellets so obtained were washed gently two to three times with culture medium, suspended in culture medium, gently triturated with a fire-polished Pasteur pipette and plated onto round glass coverslips (Fisher), which had been previously treated with poly-L-lysine (0.5 mg ml^{-1}), in small Petri dishes (35 × 12 mm). Cells were then placed in a 37 °C incubator in a 95% air/5% CO_2 atmosphere. Cells were used 2–4 d after plating.

Behavioral tests. Adult male Sprague-Dawley rats (180–230 g, 7–8 weeks) and C57BL/6J mice (18–23 g, 8–10 weeks) (Orient Bio) were used for behavioral pain tests. These animals were housed in a controlled environment, on a 12-h light/dark cycle, with free access to food and water. Experiments were carried out in accordance with the Ethical Guidelines of the International Association for the Study of Pain. Carrageenan (2% (wt/vol), 50–100 μl) was injected intradermally into the plantar surfaces of right hindpaws. Vehicle or mefloquine (40 mg per kg) were administered intraperitoneally 1 h before the tail-flick test or the Hargreaves test. All behavioral tests were conducted blinded to genotype and treatment.

For the Hargreaves test, a radiant heat stimulus was applied to the plantar surface and paw withdrawal latency was measured using a standard apparatus (Ugo Basile Biological Research Apparatus). For the tail-flick test, we measured tail reflex times to infrared heating using a Tail Flick Analgesy Meter (Ugo Basile Biological Research Apparatus). A cut-off time of 20 s was used to avoid tissue damage. For tail immersion, we measured the times taken for mice to remove their tails from a hot water bath (50–54 °C). A cut-off time of 1 min was used to avoid tissue damage. For the Randall Selitto test, a blunt conical probe was applied to the dorsal surface of the affected hindpaw of rats using an Analgesimeter (Ugo Basile Biological Research Apparatus). Probe pressure was continuously increased at 32 g s^{-1} until vocalization or a withdrawal reflex occurred. Probe pressures that elicited responses were measured in grams. For the Von Frey test, rats or mice were placed individually in a transparent plastic box with a mesh floor. Affected hindpaws were contacted with Von Frey filaments (Stoelting). Each filament was applied five times to the plantar surface of the right hind paw in an ascending order of force. The withdrawal reflex of at least three of the five applications was defined as a positive response.

Immunofluorescent staining. Immunofluorescent staining of DRGs for ANO1, TRPV1, NFM, IB4 or CGRP was performed as previously described[25]. Briefly, dissected mouse DRGs from wild-type, systemic knockout, CKO and siRNA-treated mice were sectioned on a cryostat at 10 μm and fixed in methanol. Sections were washed, incubated with blocking buffer (4% (wt/vol) bovine serum albumin in phosphate buffered saline with Twin 20) for 30 min, and with either monoclonal rabbit antibody to mouse ANO1 (ab64085, Abcam, 1:50) or polyclonal guinea pig antibody to TRPV1 (AB5566, Millipore, 1:500 in blocking solution) overnight at 4 °C. Samples were then washed and incubated with Alexa Fluor 594–conjugated donkey antibody to rabbit (A21207, Molecular Probes, 1:400) or FITC-conjugated donkey antibody to guinea pig (AP193F, Millipore, 1:400) at room temperature for 1 h. Labeled DRG sections were imaged using Leica TCS confocal system (Leica Microsystems). Goat antibody to CGRP (sc-8856, Santa Cruz), and monoclonal mouse antibodies to NFM (sc-51683, Santa Cruz) and IB4 (I21411, Invitrogen) were diluted 1:50–200 in blocking solution.

Whole-cell and single-channel current recordings. Whole-cell current and single-channel current recordings were obtained using either a voltage-clamp or a current-clamp technique with an Axopatch 200B amplifier (Molecular Devices). Whole cells were formed after breaking the plasma membrane under the pipette tips. Resistance of glass pipettes was about 3 mΩ. Junctional potentials were canceled to zero. Unless otherwise stated, bath and pipette solutions contained 140 mM NMDG-Cl, 2 mM $MgCl_2$ and 10 mM HEPES, adjusted to pH 7.2. For anion selectivity experiments, the NMDG-Cl in the control bath solution was replaced with equimolar concentration of NaCl, NaI, NaBr, $NaNO_3$ or NaF. Whole-cell currents were amplified and stored in a personal computer after digitization using Digidata 1440 (Molecular Devices). The perfusion solution was heated using a Warner TC-344B heater (Harvard Instruments). Temperatures were increased at the rate of 1–2 °C s^{-1}.

Determination of Q_{10} and activation energy. Q_{10} and the activation energy (E_a) were used to characterize the temperature dependence of ANO1 channel current. Q_{10} is a measure of relative change in a parameter for every 10° increase in temperature. An Arrhenius plot was obtained by plotting the common logarithm of the currents against reciprocal of the absolute temperature. E_a was expressed using the slope of regression line: $-E_a = \frac{2.303R\log_{10}(I_2/I_1)}{1/T_2 - 1/T_1}$, where I_2 and I_1 are the current magnitudes at higher (T_2) and lower (T_1) temperatures, respectively, and R is the gas constant (8.314 J K^{-1} mol^{-1}). Q_{10} values were determined using $Q_{10} = \exp\frac{10E_a}{RT_1T_2}$ (refs. 26,27).

Statistical analysis. All data are expressed as means ± s.e.m. Analyses were performed with GraphPad Prism version 4.03.software. To compare the differences in more than two groups, one-way ANOVA was used, followed by Tukey's *post hoc* test. Two groups were tested for statistical significance using a Student's unpaired two-tailed *t*-test. Statistical significance was accepted for $P < 0.05$.

46. Koo, J.Y. *et al.* Hydroxy-alpha-sanshool activates TRPV1 and TRPA1 in sensory neurons. *Eur. J. Neurosci.* **26**, 1139–1147 (2007).

doi:10.1038/nn.3111